1

Investigations of the Many Distinct Types of Auroras

Christopher A. Colpitts

ABSTRACT

In this chapter, the many distinct types of auroras are introduced and briefly explained. Background is given on auroral studies throughout history, and the broad categories of diffuse and discrete aurora are explained. The field-aligned current system, auroral acceleration regions, and auroral oval are introduced. The diffuse aurora, and the pitch angle diffusion resulting from wave−particle interactions that generate the diffuse aurora are then covered more extensively, including more recent investigations. The two primary acceleration mechanisms that generate the discrete aurora, inverted-V acceleration and Alfvénic acceleration, are examined in detail. Temporal changes in the aurora, particularly over the course of an auroral substorm, are the subject of the next section, followed by small-scale deformations of auroral arcs such as curls, folds, spirals, omega bands, and streamers. Finally, investigations of localized aurora that deviate from the classic auroral oval are presented, such as cusp aurora, detached dayside aurora, and evening corotating patches.

1.1. OVERVIEW

Study of the *Aurora Borealis*, also known as "northern lights" (and *Aurora Australis*, also known as "southern lights"), the extraordinarily dynamic light displays seen in the high latitudes near 70° geomagnetic latitude, dates back before recorded history. Early recorded attempts to explain the phenomenon included Hippocrates in the 5th century B.C., who was among the first to offer the theory of reflected sunlight, an incorrect theory that would persist into the modern era, as well as Roman and Chinese writings from the same era [*Eather*, 1980]. The advent of ground-based all-sky auroral imagers, and the space age that followed with its satellite-borne imagers and particle detectors, has allowed us to understand the aurora at both macroscopic and microscopic levels in terms of basic plasma physics theory. The visible auroras are actually emissions occurring in the layer of Earth's upper atmosphere called the *ionosphere*, a region at altitudes of ~ 85−600 km (depending on a variety of factors ranging from time of day to phase of solar cycle, and further divided into distinct ionospheric layers at different altitudes), where the density of charged particles rises sharply. The emissions are caused when energetic charged particles from Earth's magnetosphere penetrate into the ionosphere and transfer some of their energy to the (ionospheric) ions through collisions. Bound electrons of these ions thereby move to higher energy states, and it is the transition from the excited state back down to a more stable energy state that releases the photons that we see as visible aurora. There are different ways through which magnetospheric particles can enter the ionosphere, and as one would expect, these different processes result in distinct types of visible aurora.

The two primary processes by which magnetospheric electrons enter the ionosphere are through pitch angle

School of Physics and Astronomy, University of Minnesota, Minneapolis, Minnesota, USA

Auroral Dynamics and Space Weather, Geophysical Monograph 215, First Edition.
Edited by Yongliang Zhang and Larry J. Paxton.

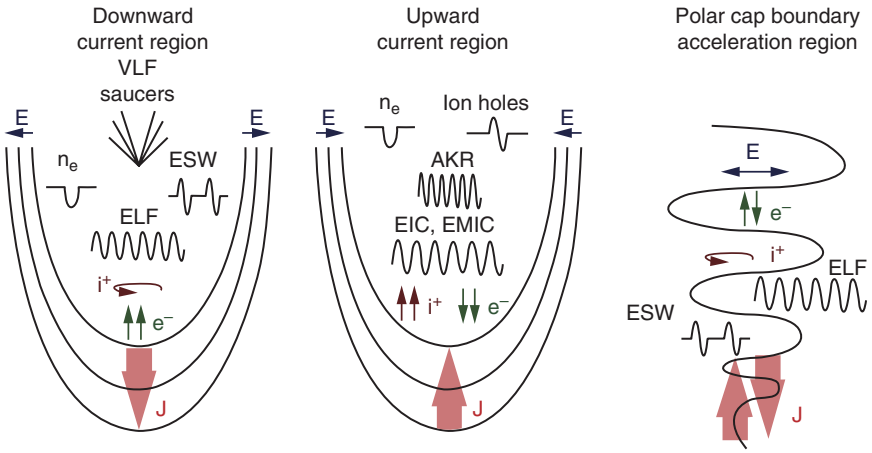

Figure 1.1 The three primary auroral acceleration regions, modified from *Paschmann et al.* [2003], which was modified from *Carlson et al.* [1998].

diffusion, which generates the diffuse aurora, and through acceleration along magnetic field lines, which generates the discrete aurora. There are multiple acceleration mechanisms; the primary two are (1) quasistatic acceleration by a parallel potential drop, which accelerates electrons in an "inverted-V" distribution at a roughly constant energy, generating aurora that is typically observed as a narrow, static east-west aligned arc; and (2) Alfvénic (named after the Swedish electrical engineer and plasma physicist Hans Alfven, 1908–1995) acceleration by the electric field of Alfvén waves, which accelerates electrons in a broadband distribution at a wide range of energies, generating more dynamic shorter-lived auroral forms. These processes, and the types of aurora generated by them, vary in a number of ways that allow us to identify and study them. For example, pitch angle diffusion can also cause magnetospheric protons to precipitate into the ionosphere. These protons then excite neutral hydrogen atoms through charge exchange collisions, thus generating the diffuse proton aurora, as well as producing secondary electrons that precipitate and add to the electron aurora [*Donovan et al.*, 2012]. There are also a number of other auroral generation mechanisms, which in turn generate their own distinct types of aurorae [*Frey*, 2007].

The observation of the aurora from the ground, and more recently from satellite-borne detectors and auroral sounding rockets, has allowed scientists to categorize different types of auroras. Auroral configurations vary in many ways, including longitudinally, latitudinally, and temporally. Longitudinally, auroras vary in local time; premidnight auroras tend to be observed in discrete arcs, while postmidnight auroras are more irregular and can include pulsating auroras, discrete arcs, and diffuse auroras [*Akasofu*, 1964; *Elphinstone et al.*, 1996].

The latitudinal variation of the aurora is typically determined by the distinct accelerating mechanisms in different regions. These mechanisms arise from different particle distributions and current structures in the acceleration regions. Earth's polar large-scale field-aligned current system was first identified by *Birkeland* [1908], and the full spatial distribution and characteristics were classified by *Iijima and Potemra* [1976], with region 1 current flowing down into the ionosphere at high latitudes on the duskside (low latitudes on dawnside) and region 2 current flowing up from the ionosphere at lower latitudes on the duskside (higher on the dawnside). This current system and the characteristics of the regions were confirmed in situ by the NASA small explorer satellite FAST (the Fast Auroral SnapshoT mission) [*Carlson et al.*, 1998].

There are three general auroral acceleration regions, as shown in Figure 1.1, which vary latitudinally: the upward current region (region 2 on the dawnside as in this figure) with converging electric field structures, large-scale density cavities, downgoing "inverted-V" electrons, upgoing ion beams, and ion conics; the downward (region 1) current region with diverging electric field structures, small-scale density cavities, upgoing field-aligned electrons and ion heating transverse to the magnetic field; and the polar cap boundary acceleration region (Alfvén wave acceleration mechanism) with variable currents, Alfvénic electric field, no density cavities, counterstreaming electrons, ion heating transverse to the magnetic field, and intense ion outflow [*Carlson et al.*, 1998; *Paschmann et al.*, 2003].

Finally, the aurora varies temporally as plasma conditions evolve, specifically at different stages within a substorm. *Akasofu* [1964] first described the temporal evolution of the aurora and introduced the concept of the substorm, and *Elphinstone et al.* [1996] expanded on this picture in a substorm review paper. Observation of these various types of auroras from the ground has led to a generally accepted picture of the auroral oval, including the latitude, longitude,

and time dependence. Further investigation using satellite particle data has given us a deeper understanding of the specific mechanisms for the generation of the different types of auroras [e.g., *Chaston et al.*, 2002; *Sadeghi et al.*, 2011]. Only very recently have we been able to combine ground-based observations with simultaneous in situ data on the same field lines to verify these generation mechanisms, including differentiating between Alfvénic and quasistatic aurora using both satellite particle data in the acceleration region and ground-based auroral images [e.g., *Chaston et al.*, 2010, 2011; *Colpitts et al.*, 2013].

1.2. DIFFUSE AURORA

When people think of the aurora, they tend to think of the dynamic visual display associated with the breakup of auroral substorms, and the distinct discrete forms generated by particle acceleration. However, the primary mechanism for generating the large-scale aurora that gives the auroral oval its characteristic shape (as seen in Figure 1.2), as well as the far more energetically important auroral generation mechanism, has long been known to be electron (and to a far lesser extent ion) pitch angle diffusion [e.g., *Jorjio* 1959; *Lui et al.*, 1977]. The location of the auroral oval is well established as being the region where the magnetic field lines map to the plasmasheet [*Evans and Moore*, 1979] and *Meng* [1979] even found the electron distributions of diffuse precipitating auroral electrons to be roughly identical to those of the trapped plasmasheet electrons.

The primary means for pitch angle diffusion of magnetospheric particles is thought to be wave−particle interaction through the cyclotron resonance [*Kennel and Petschek*, 1966]. However, the exact nature and location of this interaction, and how it changes with time, remains an open question and the diffuse aurora remains a very active area of study. The current NASA dual-satellite mission Van Allen Probes (VAP) could provide new information on these important processes [e.g., *Fennell et al.*, 2014]. Recent investigations include the role of upper band chorus in addition to the electron cyclotron harmonic waves [*Meredith et al.*, 2009; *Thorne et al.*, 2010], variation of the pitch angle scattering rate to better explain the structure of the aurora during a storm [*Chen and Schultz*, 2001], correlation of dayside whistler mode waves with the diffuse aurora [*Nishimura et al.*, 2013a] and the role that whistler waves themselves may play in the pitch angle diffusion and scattering of the magnetospheric electrons [*Horne et al.*, 2003].

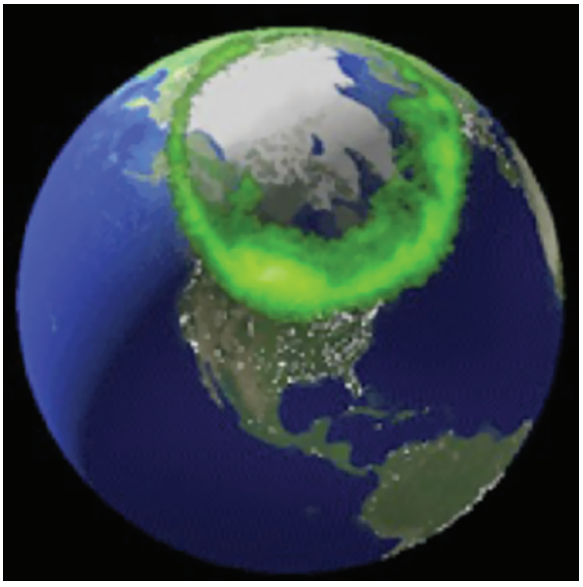

Figure 1.2 Artist's rendering of the Northern Hemisphere Auroral Oval. (Credit: NASA.)

1.3. DISCRETE AURORA

Our understanding of auroral acceleration mechanisms has improved significantly in recent years. Both Alfvén waves and inverted-V acceleration have been shown to be prevalent mechanisms for accelerating precipitating electrons into Earth's ionosphere. The quasistatic inverted-V type acceleration associated with auroral arcs was first established in the early years of satellite research [*Evans*, 1968, 1974; *Mozer and Fahleson*, 1970; *Frank and Ackerson*, 1971; *Gurnett and Frank*, 1973] and has continued to be refined in the years since [*Whipple*, 1977; *Mozer et al.*, 1977, 1980, 1998; *Ergun et al*., 1998, 2000, 2001; *McFadden et al*., 1998, *Dombeck et al*., 2013].

It was later found that in addition to quasistatic acceleration, the process of Alfvénic acceleration must also be invoked in order to explain all of the characteristics of auroral observations. [*Johnstone and Winningham*, 1982; *McFadden et al*., 1986, *Clemmons et al*., 1994; *Lynch et al*., 1994, 1999; *Knudsen et al*., 1998; *Wygant et al*., 2000, 2002; *Chaston et al*., 1999, 2000, 2002; *Dombeck et al*., 2005].

1.3.1. Quasistatic Acceleration and Auroral Arcs

Auroral arcs are the most recognizable and common type of discrete aurora, and a great deal of research has gone into their study. The so-called inverted-V electron precipitation that generates them was first identified by *Frank and Ackerson* [1971]. The inverted-V structures are always found in regions of upward field-aligned currents (see Figure 1.1), and it is the potential drop associated with this region that accelerates the electrons down the magnetic field lines into Earth's ionosphere [e.g,, *Evans*, 1974; *Mozer et al*., 1980, *Cattell et al.*, 1979, 1982]. When a current density is required on a flux tube that is beyond the carrying capacity of the plasma due to thermal drift, the particles must be accelerated to support the current, and a quasistatic

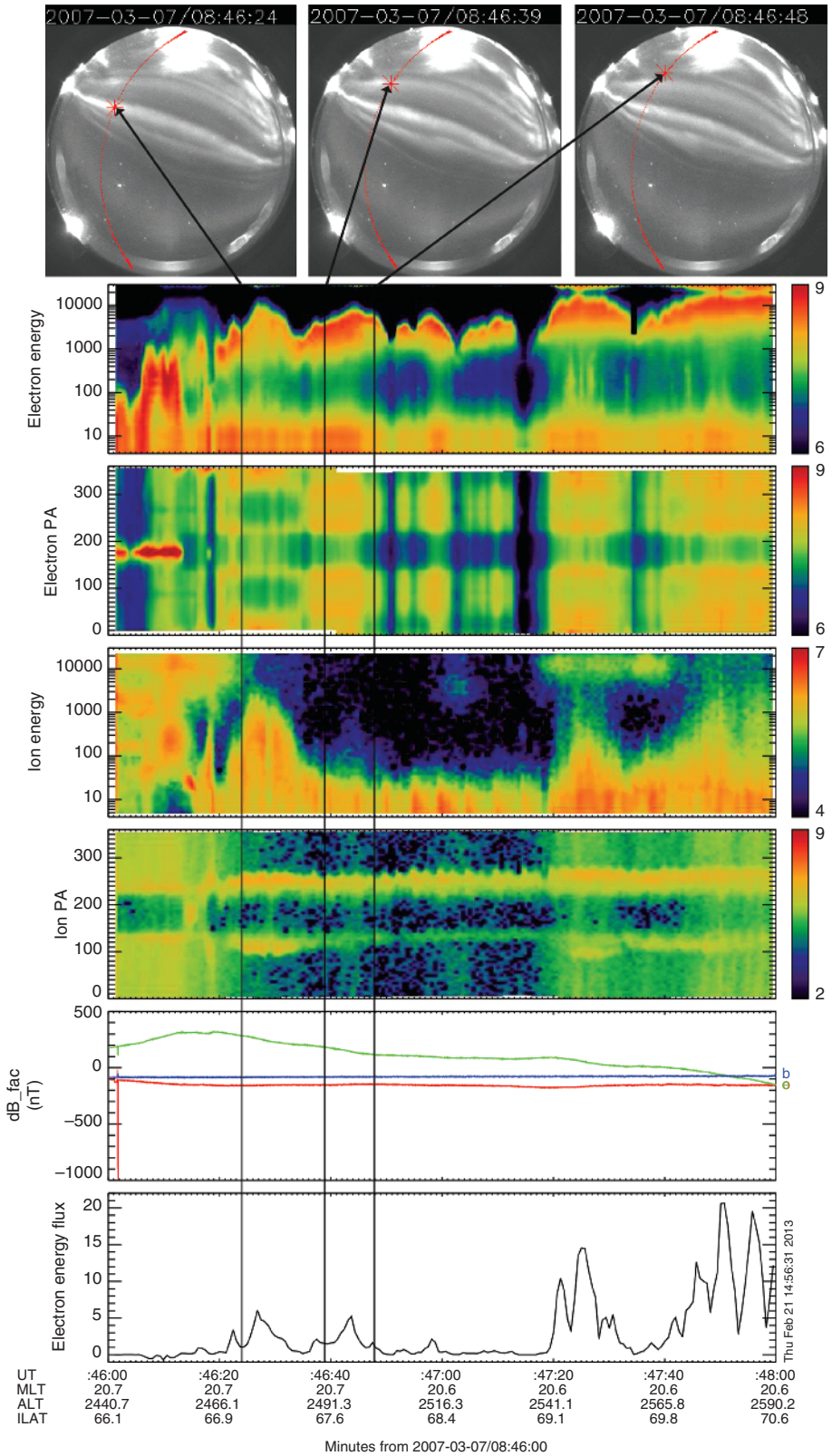

Figure 1.3 Example of inverted-V acceleration and the resulting aurora, reprinted from *Colpitts et al.* [2013]. Top panels: KIAN images for 08:46:24, 08:46:39, and 08:46:48 UT with mapped FAST trajectory (red line) and location (red star) overplotted. Lower panels: FAST data from 08:46–08:48 UT, with black vertical lines representing the times of the KI–south (red line), AN images; magnetometer panel (second from bottom) shows perturbations in the north east–west (green) and vertical (blue) directions.

potential structure with a parallel electric field develops [*Knight*, 1973; *Mozer and Hull*, 2001].

This parallel electric field in the upward current region allows hot magnetospheric electrons to be accelerated into the ionosphere, and gives them their characteristic inverted-V configuration (when viewed as an energy–time spectrogram) or "horseshoe"/"shell" (when viewed as particle distributions in energy space) shape [*Evans*, 1974; *Chiu et al.*, 1983; *McFadden et al.*, 1999]. The precise generation mechanism of these inverted-V structures has been thoroughly examined over the last several decades [e.g., *Lin and Hoffman*, 1979; *Lyons*, 1981; *Marklund et al.*, 2011], but remains an open question in the field, although it is widely believed that the field-aligned current system shown in Figure 1.1 and the Alfvén waves that arise from these currents are crucial to their development [*Borovsky*, 1993; *Luizar et al.*, 2000; *Newell et al.*, 2012; *Dombeck et al.*, 2013].

Figure 1.3 (reprinted from *Colpitts et al.* [2013], Figure 2) shows a typical example of inverted-V electron acceleration in the upward current region generating auroral arcs. The top panels in Figure 1.3 show images from the KIANA all-sky imager, part of the THEMIS (Time History of Events and Macroscale Interactions during Substorms) ground-based observatory suite, with the superimposed track of the FAST auroral satellite and its mapped location (using Tsyganenko-96 plus IRGF model) at a few specific times while it is passing over the auroral arcs. The lower panels show FAST particle and magnetic field perturbation data with the vertical black lines indicating the times of the THEMIS images.

Several discrete auroral arcs are visible in the THEMIS images as white light bands stretching roughly east–west. These arcs are also evident as peaks in the electron energy spectrogram and electron energy flux (panels 1 and 6, respectively) in the FAST data. These are the inverted-V electrons, with peak energy ~5–10 keV (corresponding to a 5000–10,000-V parallel potential drop in the acceleration region), which are accelerated downward in the upward current region and are known to produce discrete auroral arcs. This is confirmed by the THEMIS images. The first inverted-V peak corresponds to the bright arc shown in the 8:46:24 UT KIAN image, and the second peak corresponds to the second arc structure, seen in the KIAN images at 8:46:39 and 8:46:48 UT. There are four more inverted-V peaks in the FAST electron spectrogram data, which probably correspond to the next few fainter auroral arcs.

The magnetic field perturbation shown in panel 5 is referred to as a *paired sheet-like current structure*, which is typical of premidnight auroral arcs. The north–south component of the magnetic field perturbation is nearly constant (aside from small variations that do not play a role in the large-scale current structure), while there is a large perturbation in the east–west component (green line), consistent with a field-aligned current sheet extensive in longitude. As FAST goes from low latitude to high latitude in the nightside region, the perturbation first increases as the satellite passes through the downward current sheet (region 2 on the duskside as in this figure) and then decreases as FAST passes through the upward current sheet (region 1). Throughout the downward current region, FAST maps to a dark area in the all-sky images, consistent with expected lack of visible aurora in the downward current region.

The FAST electron distributions for the times of the three KIAN images from Figure 1.3 are shown in Figure 1.4, with parallel and perpendicular energy in log scale on the x and y axes and the log of the energy flux in color scale. At all 3 times the distribution shows the characteristic horseshoe shape associated with quasistatic inverted-V acceleration, with a single loss cone in the upgoing component and a narrow band of electrons in the other directions at the energy of the parallel potential drop.

1.3.2. Alfvénic Aurora

Alfvénic acceleration occurs when the scale size of Alfvén waves perpendicular to the background magnetic field is small enough for kinetic effects to be important. When this occurs, the wave electric field has a component parallel to the magnetic field, which can accelerate electrons [*Chen and Hasagawa*, 1974; *Goertz and Boswell*, 1979; *Lysak and Lotko*, 1996; *Lysak*, 1998]. Refinement of the understanding of this process has also continued in the subsequent years through observation [*Dombeck et al*, 2005; *Chaston et al*., 2007; *Nakajima et al*., 2007], theory [*Lysak and Lotko*, 1996; *Lysak and Song*, 2003] and simulation [*Kleitzing and Hu*, 2001; *Chaston et al*., 2002; *Ergun et al.*, 2002; *Chen et al*., 2005].

Figure 1.5 shows a typical example of Alfvénic aurora, observed intermittently and perhaps simultaneously with inverted-V aurora, with images from the Inuviak all-sky imager along with data from FAST, in the same format as Figure 1.3. In this case the INUV images show distorted aurora, with bright spots and some arcs, including a brightening discrete east–west-aligned arc in the northern portion of the field of view. The FAST data show periods of both inverted-V acceleration (14:52:05–14:52:35, 14:53:20–14:53:30 – marked by blue shaded regions in the figure which show times of upward currents, positive slope to the green line in the panel below showing dB) and broadband electron precipitation associated with Alfvénic acceleration (14:52:40–14:53:12, 14:53:32–14:53:36 – pink shaded region during times of downward or mixed currents).

The inverted-V's in this case have peak energy ~1–3 keV (corresponding to a 1000–3000-V parallel potential drop

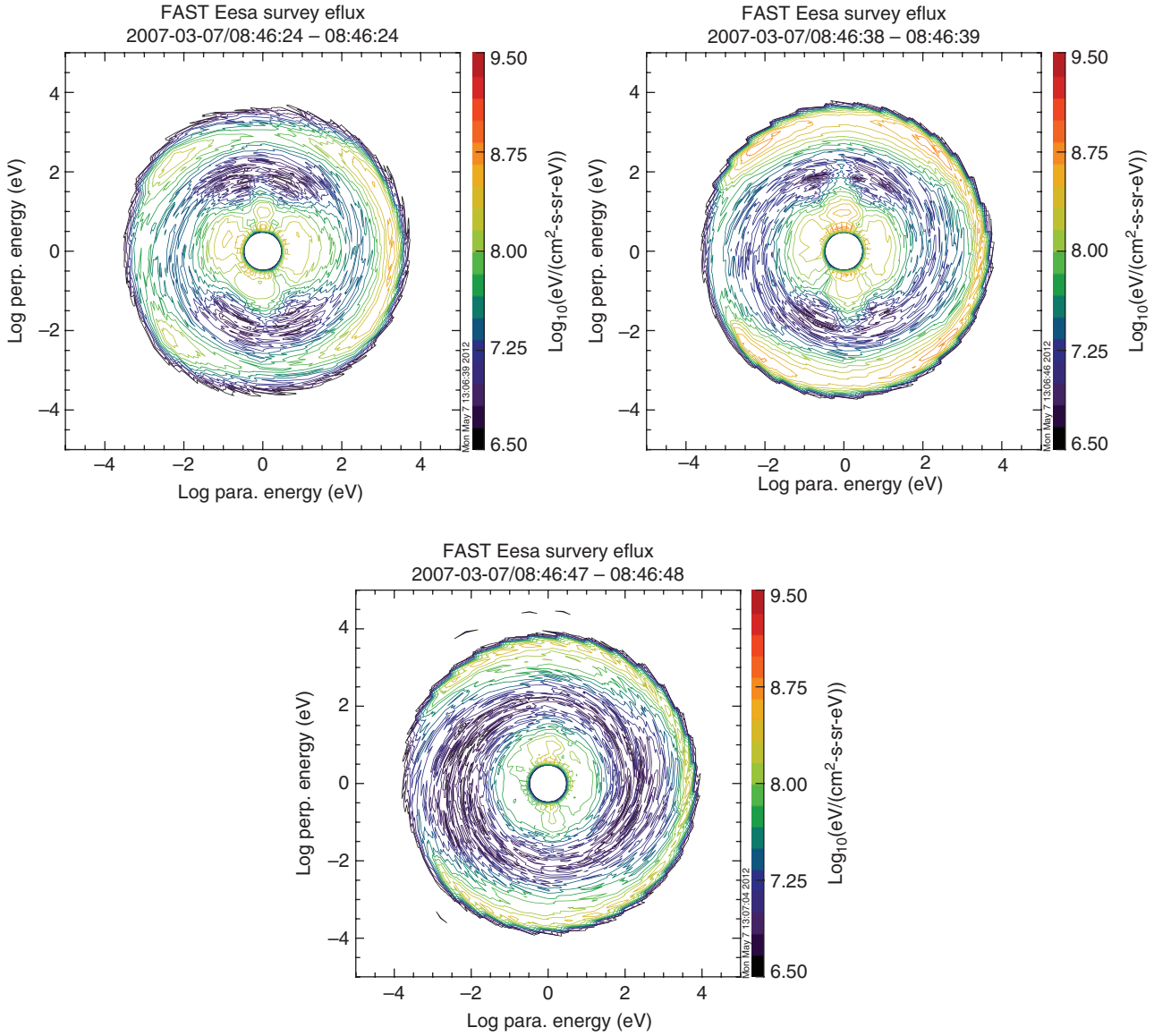

Figure 1.4 FAST electron energy distributions for 08:46:24, 08:46:39, and 08:46:48 UT with parallel energy in log scale on the *x* axis, log perpendicular energy on the *y* axis, and log energy flux in color scale, reprinted from *Colpitts et al.* [2013].

in the acceleration region). In this event there is a N-S (red line) perturbation comparable to the E-W (green) component, consistent with a more complex current system including current sheets, twisted currents, and possibly line currents. Note that even these smaller scale inverted-V electrons are always accelerated downward in an upward current region, as can be seen in the pitch angle spectrogram and the magnetic field perturbation (in this case the satellite is moving equatorward in the dawnside, so an increasing east−west perturbation corresponds to the upward current region).

In the THEMIS images the single faint discrete arc in the northern portion of the field of view, extensive in longitude but with narrow spatial scale in latitude, and temporally remaining stable before brightening, is consistent with auroral forms associated with inverted-V acceleration, while the dynamic, amorphous nature of the remaining aurora in the images is typical of the spatial and temporal evolution of aurora associated with Alfvénic acceleration [*Chaston et al.,* 2010, 2011]. The altitudinal extent of the auroral forms cannot be determined from these 2D images, but this has also been studied extensively and in particular auroral rays that extend in altitude are associated with Alfvénic acceleration [*Ivchenko et al.*, 2005]. There is an inverted-V peak around the time of the 14:53:27 UT INUV image, when the FAST satellite maps close to the faint

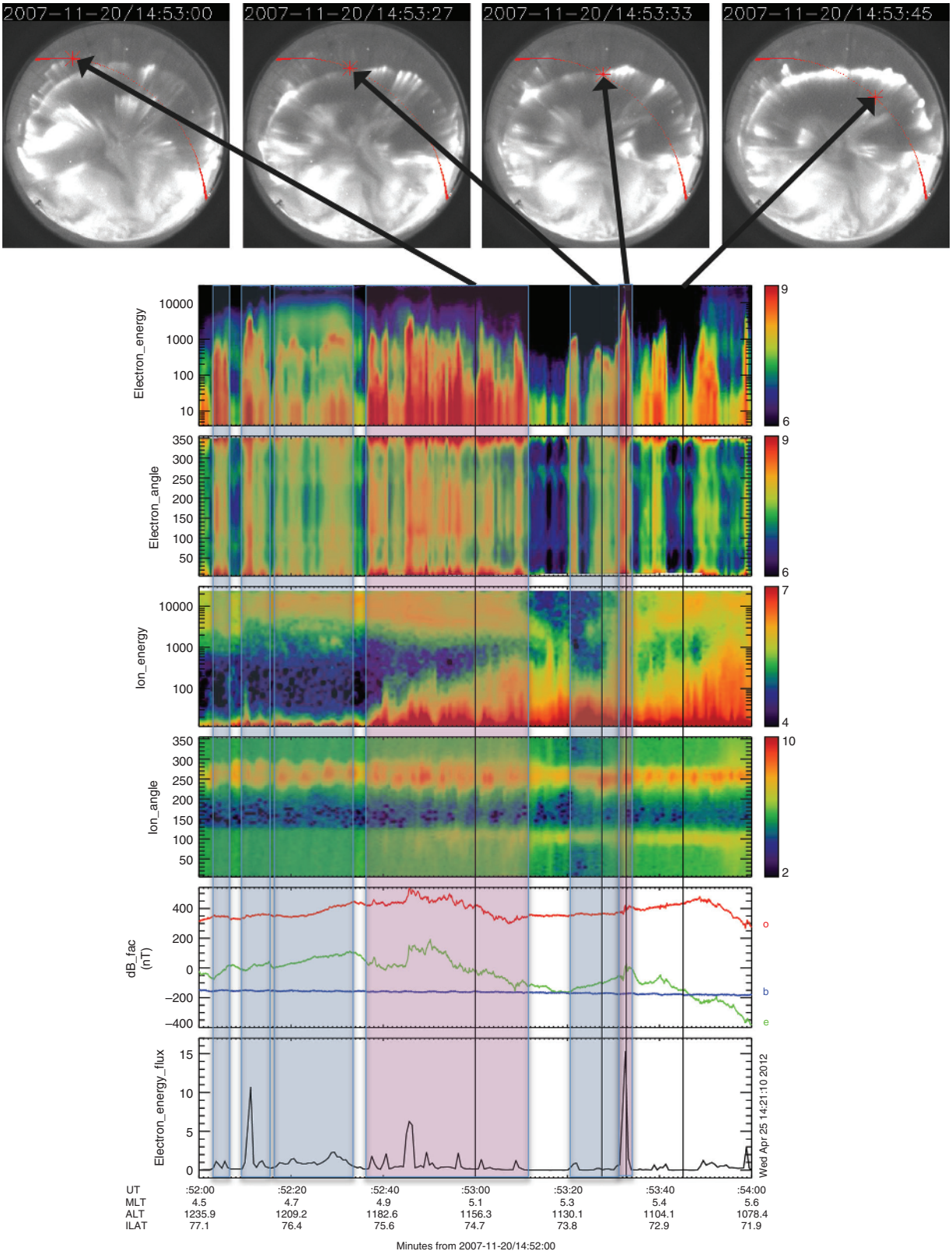

Figure 1.5 Example of Alfvéenic acceleration and the resulting aurora, reprinted from *Colpitts et al.* [2013]. Top panels: INUV images for 14:53:00, 14:53:27, 14:53:33, and 14:53:45 UT with mapped FAST trajectory (red line) and location (red star) overplotted. Lower panels: FAST data from 14:52–14:54 UT with black vertical lines representing the times of the INUV images; magnetometer panel (second from bottom) shows perturbations in the north–south (red line), east–west (green) and vertical (blue) directions.

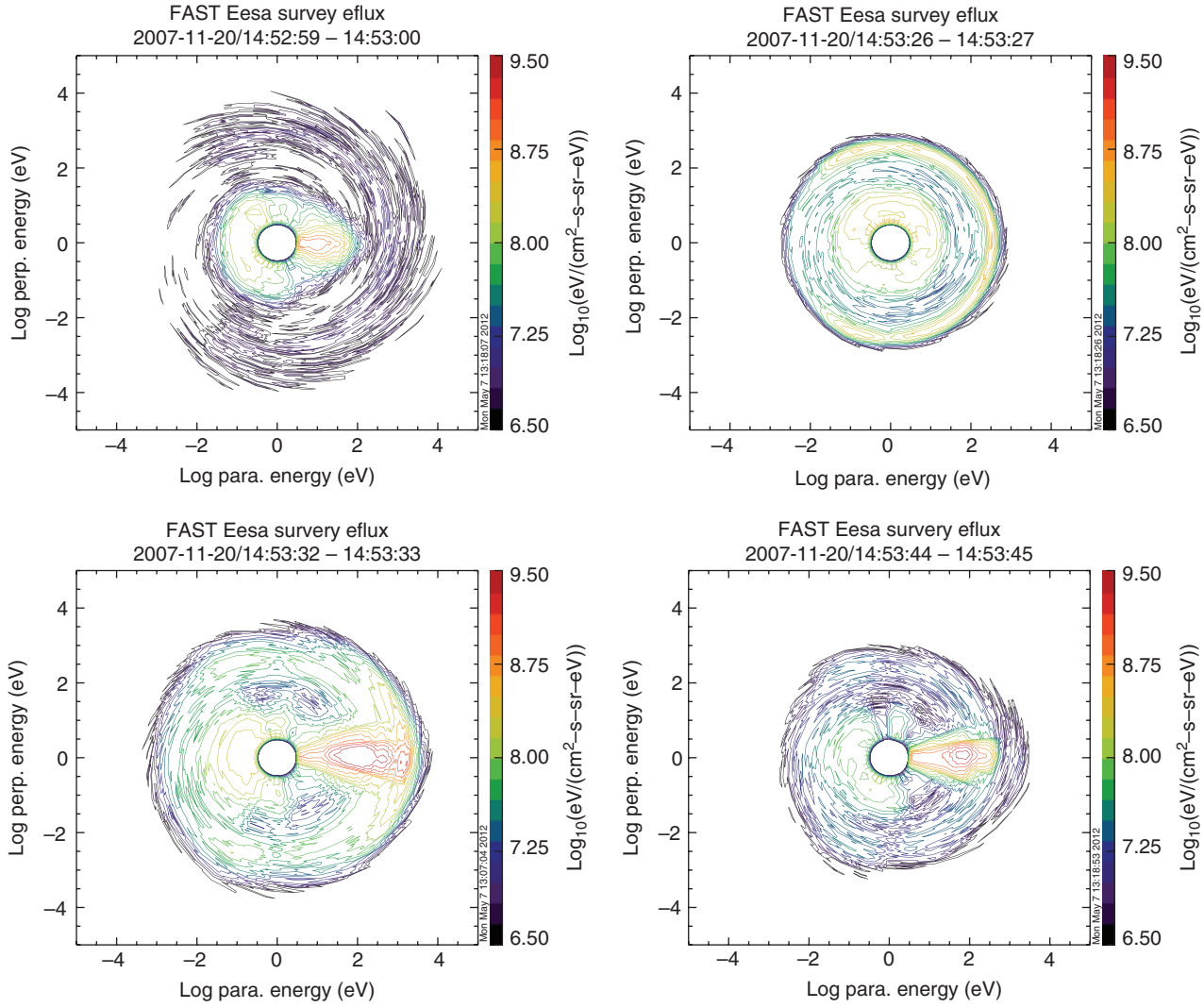

Figure 1.6 FAST electron energy distributions for 14:53:00, 14:53:27, 14:53:33, and 14:53:45 UT, with parallel energy in log scale on the *x* axis, log perpendicular energy on the *y* axis, and log energy flux in color scale, reprinted from *Colpitts et al.* [2013].

discrete arc, while the other images correspond to times of Alfvénic aurora. The many other inverted-V peaks in the FAST electron spectrogram data could correspond to other arcs and bright spots visible in the INUV image, but the aurora at this time was more dynamic than shown in Figure 1.3, so the peak that FAST went through at those times may not be visible in the INUV images from this time.

The electron distributions for the four times during the INUV observations from Figure 1.5 are shown in Figure 1.6. The top left panel, from the time of the first INUV image, shows low-energy downgoing electrons typical of Alfvénic acceleration, consistent with FAST mapping to the somewhat bright but amorphous aurora in the INUV image. The top right panel is from the second INUV image when fast mapped to the faint narrow discrete arc and shows the horseshoe distribution typical of inverted-V acceleration; the extreme difference in these top two panels for times when FAST passes through what could appear to be similar features in the all-sky images show the benefit of combining in situ particle measurements with ground based imagers. The third and fourth panels show very intense fluxes of downgoing broadband electrons associated with Alfvénic acceleration at the times of the third and fourth INUV images. There is little evidence of inverted-V acceleration at these times; while there are some higher-energy electrons at all pitch angles aside from the upgoing component, they are not narrow-banded as would be expected for acceleration from a quasistatic potential drop, and as is seen in the other horseshoe distributions.

1.4. DYNAMIC AURORA AND SMALL-SCALE AURORAL STRUCTURES

1.4.1. Modification of the Large-Scale Auroral Oval

The general structure of the auroral oval has been known for decades, first established by ground-based observations [*Akasofu*, 1964] and later confirmed through satellite observation [e.g., *Anger et al.*, 1973; *Akasofu*, 1974]. The oval itself, however, is quite dynamic. The boundaries of the auroral oval change seasonally [*Meng*, 1979], and with geomagnetic conditions such as the interplanetary magnetic field [*Jayachandran et al.*, 2008] and ring current intensity [*Milan et al.*, 2009]. The most extensively studied variation of the auroral oval is that associated with auroral substorms, which also produce many of the common discrete auroral forms.

Figure 1.7 shows an illustration from *Akasofu* [1964] that shows the evolution of the auroral oval during a substorm.

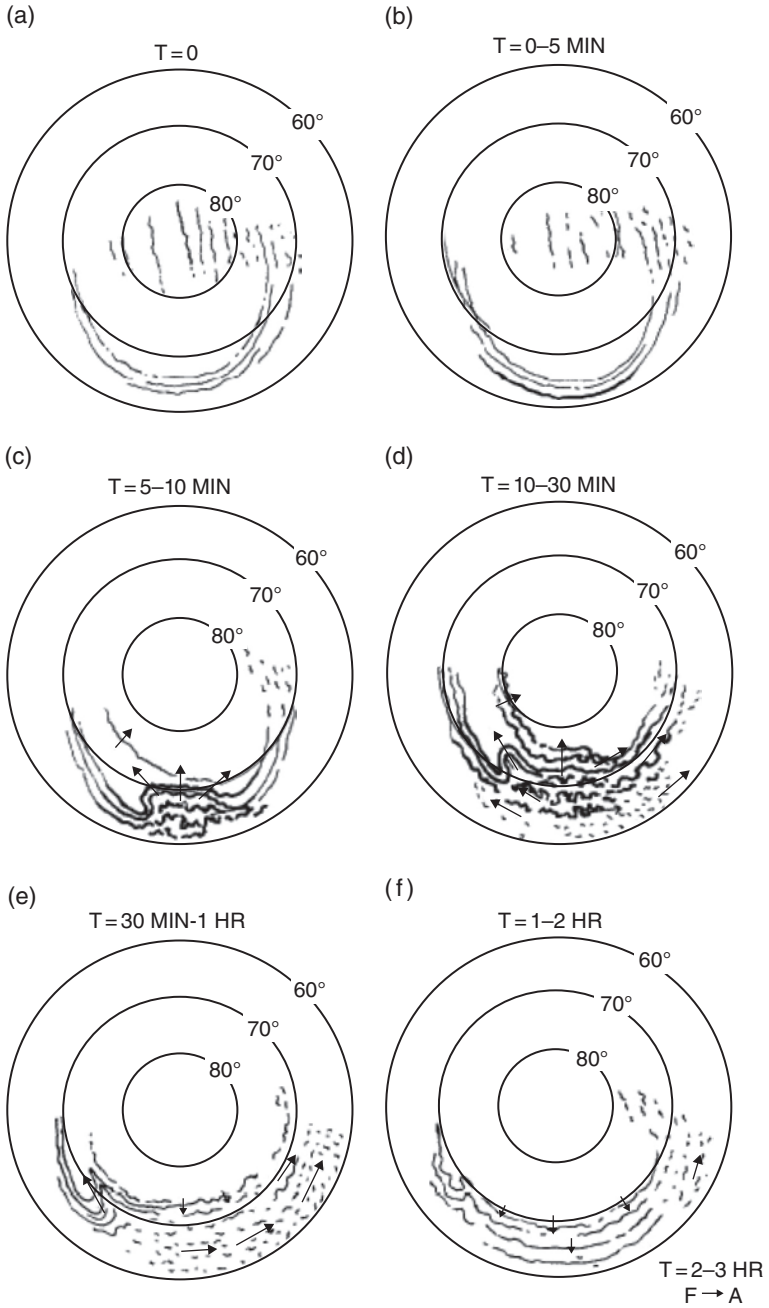

Figure 1.7 Illustration from *Akasofu* [1964] showing the stages of a typical auroral substorm: (a) Quiet phase; (b,c) and (d) expansive phase; (e,f) recovery phase.

The first panel represents the quiet phase, characterized by faint arcs extending east-west. The second, third, and fourth panels are the expansive phase, which involves a brightening of one or more arcs, followed by a poleward motion and sometimes a bulge in the midnight sector. The bottom two panels represent the recovery phase, characterized by diffuse aurora moving equatorward and eastward and the reestablishment of faint discrete arcs. This has remained the canonical model of the auroral substorm in the decades since, but there have been many additions and improvements, and we know now that every substorm is different.

Early improvements to the substorm model included the addition of dayside aurora [*Feldstein and Starkov*, 1967], the distinction between proton and electron aurora [*Fukunishi*, 1975], and the development of the growth phase concept [*McPherron*, 1970, 1972]. Inconsistencies in the literature regarding substorms led to the 1978 Victoria conference, the results of which were presented in *Rostoker et al.* [1980], providing a consistent definition for substorms that would persist over the decades to come. *Elphinstone et al.* [1996] summarized the advances in substorm understanding up to that point, catalogued different types of substorms, and showed how satellite-borne instruments confirmed the substorm model and tied the different types of aurora to changes elsewhere in the magnetosphere. *Mende et al.* [2002, 2003] used IMAGE (Imager for Magnetopause-to-Aurora Global Exploration) and FAST observations to differentiate between main phase and recovery phase aurora, and between quasistatic and Alfvénic aurora. *Nishimura et al.* [2010, 2011] and *Mende et al.* [2011] identified the sequence of events leading to substorm onset using THEMIS all-sky imagers, showing first a poleward boundary intensification followed by an equatorward-moving north−south arc.

More recent studies have been able to combine ground-based observations with simultaneous in situ data on the same field lines to further expand on the substorm picture, allowing one to see smaller-scale structures with faster time resolution than the (earlier) comparisons with satellite imaging (Polar, IMAGE). *Zou et al.* [2010] and *Frey et al.* [2010] used THEMIS ground-based imagers (GBO) and Reimei satellite data to look for precursors to auroral substorms. Using FAST and THEMIS data, *Jiang et al.* [2012] established a preexisting auroral arc present before substorm onset. Recent discoveries using THEMIS GBO and another ground-based all-sky imager at Resolute Bay [*Nishimura et al.*, 2013b], and THEMIS GBO with radar data [*Lyons et al.*, 2011] indicate that polar cap flows and auroral streamers may play an important role in substorm onset. *Yue et al.* [2013] looked at interplanetary shocks using THEMIS spacecraft and GBO data, concluding that fast flows are the magnetotail's response to the shock front that correspond to the poleward boundary intensifications (PBIs) and auroral streamers that develop in the ionosphere. *Colpitts et al.* [2013] examined several conjunctions of THEMIS GBO and FAST to identify distinct types of aurora in both the imagers and the satellite particle and field data, and confirmed the current theory of auroral acceleration and substorm models; for example, the particle distributions observed in situ on field lines above ground-based imagers matched those expected for the type (Alfvenic, quasistatic, substorm) of aurora visible from the ground.

1.4.2. Small-Scale Deformations of Discrete Auroral Arcs

In addition to the large-scale discrete arcs and Alfvénic auroras, a great number of small-scale auroral forms have been identified and studied. *Hallinan and Davis* [1970] first identified curls, folds, and spirals, and *Wagner et al.* [1983] investigated the generation mechanisms for these three small-scale (km and 10s of km) structures, invoking shear-driven plasma instabilities such as the Kelvin−Helmholtz instability (KHI). Figure 1.8 shows some examples of auroral folds from *Wagner et al.* [1983]. The folds [*Kataoka et al.*, 2011], spirals [*Lysak and Song,* 1996; *Marklund et al.*, 1998; *Partamies et al.*, 2001; *Hu et al.*, 2013], and curls [*Vogt et al.*, 1999] continue to be active areas of study, with other generation mechanisms in addition to KHI often invoked such as the tearing instability [*Dahlgren et al.*, 2010], particularly for folds [*Chaston and Seki,* 2010] and the ion acoustic and ion cyclotron

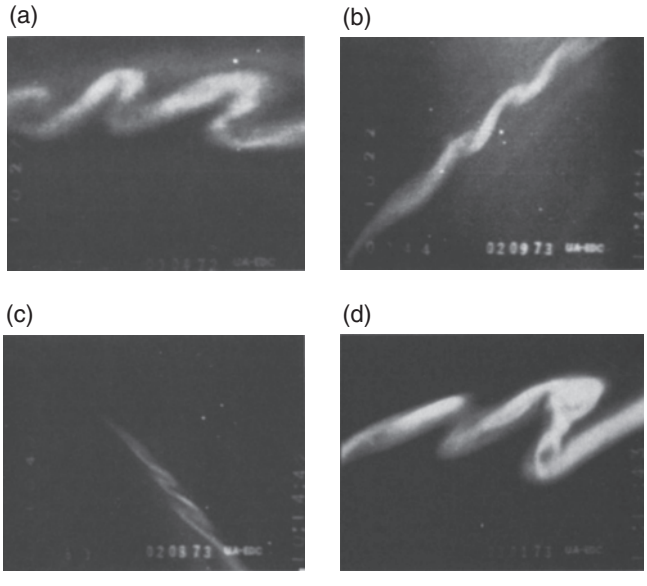

Figure 1.8 Examples of auroral folds (from *Wagner et al.* [1983]). The distinct types of anomalous localized aurora labeled in the figure are named and described in the text.

instability arising from interactions of the electron beam with an Alfvén wave [*Seyler and Liu*, 2007].

On a slightly larger (100s of km) scale, auroral omega bands, which tend to develop during the recovery phase of substorms and are so named because of their resemblance of the Greek symbol Ω (omega) and were first identified by *Akasofu and Kimball* [1964], have also been extensively studied [e.g., *Opgenoorth et al.*, 1983; *Luhr and Schlegel*, 1994]. These bands have been attributed to the shear instability of neutral winds [*Lyons and Walterscheild,* 1985] and the interchange instability between paired current sheets [*Yamamoto et al.*, 1997], and continue to be investigated as well [*Wild*, 2011]. The dark areas between auroral arcs, or black aurora, have also been the subject of extensive research [*Marklund et al.*, 1994, 1997; *Trondsen and Cogger*, 1997]. *Stenbaek-Nielsen et al.* [1998] and *Peticolas et al.* [2002] investigated fine scale auroral arc structure and black aurora with the FAST satellite and aircraft-borne cameras and imagers. The two competing mechanisms for the origin of black aurora, downward field-aligned currents causing Kelvin–Helmholtz instability [e.g., *Marklund et al.* 1997] and a magnetospheric "blocking" mechanism involving energy-dependent wave–particle interactions [*Peticolas et al.*, 2002] were investigated recently by *Archer et al.* [2011], who concluded that the magnetospheric blocking mechanism was most consistent with their observations.

Auroral streamers are small (~100s of km) short-lived north–south arcs that can occur in the auroral bulge during the expansion phase of substorms, as well as on the poleward edge of the aurora during nonsubstorm times. Study of these nonsubstorm streamers has recently gained a great deal of momentum, as they have been associated with the onset of auroral substorms, which is an extremely active research area. First identified by *Nakamura et al.* [1993] as small-scale structures within the canonical auroral bulge associated with substorm breakup (see Figure 1.7), they have since been associated with Earthward flow bursts [*Nakamura et al.*, 2001; *Liu et al.*, 2008; *Gallardo-Lacourt et al.*, 2014], poleward boundary intensifications [*Lyons et al.,* 1999; *Nishimura et al.*, 2011] and Pi2 pulsations [*Nishimura et al.*, 2012], all of which are considered indicators of substorm onset.

1.4.3. Anomalous Localized Auroral Forms

In addition to the modifications of the diffuse auroral oval and common deformations of discrete auroral arcs discussed above, numerous auroral forms deviate from the simplified model of the auroral oval. Many of these anomalous forms are catalogued in a review by *Frey* [2007] and shown in Figure 1.9, reprinted from that review. Ten different types of localized aurora are identified and labeled 1–10 in Figure 1.9. The detached dayside aurora (labeled as 1 in Figure 1.9, also called *midday subauroral patches* or *subauroral proton flashes*) was first identified by *Elphinstone et al.* [1993] and continues to be investigated [*Zhang et al.*, 2002; *Hubert et al.* 2004]. Dayside cusp aurora (2 in Figure 1.9) is associated with equatorial magnetopause reconnection, while the cusp auroral spot (3; Figure 1.9) is assumed to be the result of antiparallel reconnection at the high-latitude magnetopause [*Milan et al.*, 2000; *Sandholt et al.*, 1998; *Frey et al.*, 2002; *Fuselier et al.*, 2003].

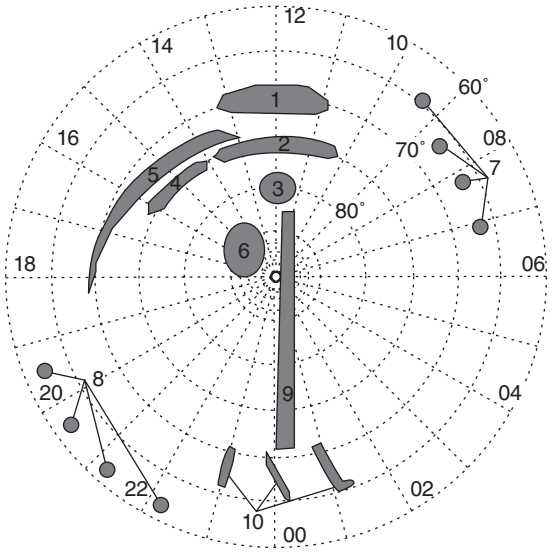

Figure 1.9 Anomalous aurora, from *Frey* [2007].

The afternoon hotspot (4; Figure 1.9) arises from the increased upward current in this region [*Liou et al.*, 1997], while the afternoon detached arcs (5; Figure 1.9) are associated with the plasmaspheric plume and generated by proton resonance with EMIC waves [*Fraser and Nguyen*, 2001]. High-latitude dayside aurora (6; Figure 1.9) results from a parallel potential that develops to balance pressure with the solar wind plasma during periods of low solar wind density [*Siscoe et al.*, 2001]. Subauroral morning proton spots (7; Figure 1.9) and evening corotating patches (8; Figure 1.9) are less well understood, although they may be generated by the plasmaspheric expansion and resulting precipitation that occur after a geomagnetic storm [*Singh and Horwitz*, 1992; *Newell*, 2003]. The mechanism behind polar cap arcs (9; Figure 1.9, also called *theta aurora*) is also still being debated [e.g., *Chang et al.*, 1998; *Kullen et al.*, 2002; *Naehr and Toffoletto*, 2004] though ionospheric flows and changes in IMF B_y have recently been shown to be good candidate mechanisms [*Fear and Milan*, 2012a,b]. Auroral streamers (10; Figure 1.9) were discussed in the previous section.

The auroras come in innumerable shapes, many specific to certain generation mechanisms and/or specific locations. It would be impossible to list them all here, but those presented above exemplify the most common and

extensively studied types of aurora that have been observed through the years. The following studies represent the latest investigations of many of these distinct types of aurora.

REFERENCES

Akasofu, S-I. (1964), The development of the auroral substorm. *Planet. Space Sci.*, *12*, 273−282.

Akasofu, S.-I., and D. S. Kimball (1964), The dynamics of the aurora—I, *J. Atmosph. Terr. Phys.*, *26*, 205–211.

Akasofu, S.-I. (1974), A study of auroral displays photographed from the DMSP-2 satellite and from the Alaska meridian chain of stations, *Space Sci Rev.*, *16*(5), 617−725.

Anger, C. D., A. T. Y. Lui, and S.-I. Akasofu (1973), Observations of the auroral oval and a westward traveling surge from the Isis 2 satellite and the Alaskan meridian all-sky cameras, *J. Geophys. Res.*, *78*(16), 3020–3026.

Archer, J., H. Dahlgren, N. Ivchenko, B. S. Lanchester, and G. T. Marklund (2011), Dynamics and characteristics of black aurora as observed by high resolution ground-based imagers and radar, *Int. J. Remote Sens.*, *32*, 2973−2985.

Birkeland, K. (1908), *The Norwegian Aurora Polaris Expedition 1902−1903,* Vol. 1, *On the Cause of Magnetic Storms and the Origin of Terrestrial Magnetism*, New York and Christiania (now Oslo): H. Aschehoug & Co.

Borovsky, J. E. (1993), Auroral arc thicknesses as predicted by various theories, *J. Geophys. Res.*, *98*(A4), 6101–6138.

Carlson, C. W., R. F. Pfaff, and J. G. Watzin (1998), The Fast Auroral SnapshoT (FAST) mission, *Geophys. Res. Lett.*, *25*(12), 2013–2016.

Cattell, C. A., R. Lysak, R. B. Torbert, and F. S. Mozer (1979), Observations of differences between regions of current flowing into and out of the ionosphere. *Geophys. Res Lett.*, *6*, 621–624.

Cattell, C. A., M. Kim, R. P. Lin, and F. S. Mozer (1982), Observations of large electric fields near the plasmasheet boundary by ISEE-1. *Geophys. Res. Lett.*, *9*, 539–542.

Chang, S.-W., J. D. Scudder, J. B. Sigwarth, L. A. Frank, N. C. Maynard, W. J. Burke, W. K. Peterson, E. G. Shelley, R. Friedel, J. B. Blake, R. A. Greenwald, R. P. Lepping, G. J. Sofko, J.-P. Villain, and M. Lester (1998), A comparison of a model for the theta aurora with observations from Polar, Wind, and SuperDARN, *J. Geophys. Res.*, *103*, 17,367–17,390.

Chaston, C. C., C. W. Carlson, W. J. Peria, R. E. Ergun, and J. P. McFadden (1999), FAST observations of inertial Alfvén waves in the dayside aurora, *Geophys. Res. Lett.*, *26*, 647.

Chaston, C. C., C. W. Carlson, R. E. Ergun, and J. P. McFadden (2000), Alfvén waves, density cavities and electron acceleration observed from the FAST spacecraft, *Physica Scripta*, *T84*, 64.

Chaston, C. C., J. W. Bonnell, L. M. Peticolas, C. W. Carlson, and J. P. McFadden (2002), Driven Alfvén waves and electron acceleration: A FAST case study, *Geophys. Res. Lett.*, *29*, 1535.

Chaston, C. C., C. W. Carlson, J. P. McFadden, R. E. Ergun, and R. J. Strangeway (2007), How important are dispersive Alfvén waves for auroral particle acceleration? *Geophys. Res. Lett.*, *34*, L07101, doi:10.1029/2006GL029144.

Chaston, C. C., K. Seki, T. Sakanoi, K. Asamura, and M. Hirahara (2010), Motion of aurorae, *Geophys. Res. Lett.*, *37*, L08104, doi:10.1029/2009GL042117.

Chaston, C. C., and K. Seki (2010), Small-scale auroral current sheet structuring, *J. Geophys. Res.*, *115*, A11221, doi:10.1029/2010JA015536.

Chaston, C. C., K. Seki, T. Sakanoi, K. Asamura, M. Hirahara, and C. W. Carlson (2011), Cross-scale coupling in the auroral acceleration region, *Geophys. Res. Lett.*, *38*, L20101, doi:10.1029/2011GL049185.

Chen, L., and A. Hasagawa (1974), A theory of long-period magnetic pulsations. 1. Steady state excitation of field line resonance, *J. Geophys. Res.*, *79*, 1024.

Chen, M. W., and M. Schulz (2001), Simulations of diffuse aurora with plasma sheet electrons in pitch angle diffusion less than everywhere strong, *J. Geophys. Res.*, *106*(A12), 28949–28966.

Chen, L.-J., C. A. Kletzing, S. H. Hu, and S. R. Bounds (2005), Auroral electron dispersion below inverted-V energies: Resonant deceleration and acceleration by Alfvén waves, *J. Geophys. Res.*, *110*, A10S13, doi:10.1029/2005JA011168.

Chiu, Y. T., M. Schulz, J. F. Fennell, and A. M. Kishi (1983), Mirror instability and the origin of morningside auroral structure, *J. Geophys. Res.*, *88*(A5), 4041–4054. doi:10.1029/JA088iA05p04041.

Clemmons, J. H., M. H. Boehm, G. E. Paschmann, and G. Haerendel (1994), Signatures of energy-time dispersed electron fluxes observed by Freja, *Geophys. Res. Lett.*, *21*, 1899.

Colpitts, C. A., S. Hakimi, C. A. Cattell, J. Dombeck, and M. Maas (2013), Simultaneous ground and satellite observations of discrete auroral arcs, substorm aurora, and Alfvénic aurora with FAST and THEMIS GBO, *J. Geophys. Res. Space Phys.*, *118*, 6998–7010.

Dahlgren, H., A. Aikio, K. Kaila, N. Ivchenko, B. S. Lanchester, D. K. Whiter, and G. T. Marklund (2010), Simultaneous observations of small multi-scale structures in an auroral arc, *J. Atmosph. Sol. Terr. Phys.*, *72*(7−8), 633–637.

Dombeck, J., C. Cattell, J. R. Wygant, A. Keiling, and J. Scudder (2005), Alfvén waves and Poynting flux observed simultaneously by Polar and FAST in the plasma sheet boundary layer, *J. Geophys. Res.*, *110*, A12S90, doi:10.1029/2005JA011269.

Dombeck, J., C. Cattell, and J. McFadden (2013), A FAST study of quasi-static structure ("Inverted-V") potential drops and their latitudinal dependence in the premidnight sector and ramifications for the current-voltage relationship, *J. Geophys. Res. Space Phys.*, *118*, 5731–5741.

Donovan, E., E. Spanswick, J. Liang, J. Grant, B. Jackel, and M. Greffen (2012), Magnetospheric dynamics and the proton aurora, in A. Keiling et al. (eds.), *Auroral Phenomenology and Magnetospheric Processes: Earth And Other Planets*, Washington, DC: American Geophysical Union (AGU), 365–378.

Eather, R. H. (1980), *Majestic Lights: The Aurora in Science, History, and the Arts*. Washington, DC: AGU.

Elphinstone, R. D., D. J. Hearn, J. S. Murphree, L. L. Cogger, M. L. Johnson, and H. B. Vo (1993), Some UV dayside auroral morphologies, in R. L. Lysak (ed.), *Auroral Plasma Dynamics*, Geophys. Monograph Series Vol. 80, Washington, DC: AGU, 31–45.

Elphinstone, R. D., J. S. Murphree, and L. L. Cogger (1996), What is a global auroral substorm? *Rev. Geophys. 34*(2), 169−232.

Ergun, R. E., C. W. Carlson, J. P. McFadden, F. S. Mozer, G. T. Delory, W. Peria, C. C. Chaston, M. Temerin, I. Roth, L. Muschietti, R. Elphic, R. Strangeway, R. Pfaff, C. A. Cattell, D. Klumpar, E. Shelley, W. Peterson, E. Moebius, and L. Kistler (1998), FAST satellite observations of large-amplitude solitary structures, *Geophys. Res. Lett.*, *25*, 2041.

Ergun, R. E., C. W. Carlson, J. P. McFadden, F. S. Mozer, and R. J. Strangeway (2000), Parallel electric fields in discrete arcs, *Geophys. Res. Lett.*, *27*, 4053.

Ergun, R. E., Y. J. Su, L. Andersson, C. W. Carlson, J. P. McFadden, F. S. Mozer, D. L. Newmann, M. V. Goldman, and R. J. Strangeway (2001), Direct observation of localized parallel electric fields in a space plasma, *Phys. Rev. Lett.*, *87*, 045003.

Ergun, R. E., L. Andersson, D. Main, Y.-J. Su, D. L. Newman, M. V. Goldman, C. W. Carlson, J. P. McFadden, and F. S. Mozer (2002), Parallel electric fields in the upward current region of the aurora: Numerical solutions, *Phys. Plasmas 9*, 3695−3704.

Evans, D. S. (1968), The observations of a near monoenergetic flux of auroral electrons, *J. Geophys. Res.*, *73*, 2315.

Evans, D. S. (1974), Precipitating electron fluxes formed by a magnetic field-aligned potential difference, *J. Geophys. Res.*, *79*, 2853.

Evans, D. S., and T. E. Moore (1979), Precipitating electrons associated with the diffuse aurora: Evidence for electrons of atmospheric origin in the plasma sheet, *J. Geophys. Res.*, *84*(A11), 6451–6457.

Fear, R. C., and S. E. Milan (2012), *J. Geophys. Res.*, *117*, A03213, doi:10.1029/2011JA017209.Fear, R. C., and S. E. Milan (2012b), *J. Geophys. Res.*, *117*, A09230, doi:10.1029/2012JA017830.

Feldstein, Y. I., and G. V. Starkov (1967), Dynamics of auroral belt and polar geomagnetic disturbances, *Planet. Space Sci.*, *15*, 209−229.

Fennell, J. F., J. L. Roeder, W. S. Kurth, M. G. Henderson, B. A. Larsen, G. Hospodarsky, J. R. Wygant, J. S. G. Claudepierre, J. B. Blake, H. E. Spence, J. H. Clemmons, H. O. Funsten, C. A. Kletzing, and G. D. Reeves (2014), Van Allen probes observations of direct wave-particle interactions, *Geophys. Res. Lett.*, *41*, 1869–1875, doi:10.1002/2013GL059165.

Frank, L. A., and K. L. Ackerson (1971), Observations of a charged particle precipitation into the auroral zone, *J. Geophys. Res.*, *76*, 3612.

Fraser, B. J., and T. S. Nguyen (2001), Is the plasmapause a preferred source region of electromagnetic ion cyclotron waves in the magnetosphere? *J. Atmosph. Sol. Terr. Phys.*, *63*, 1225–1247.

Frey, H. U. (2007), Localized aurora beyond the auroral oval, *Rev. Geophys.*, *45*, RG1003, doi:10.1029/2005RG000174.

Frey, H. U., S. B. Mende, T. J. Immel, S. A. Fuselier, E. S. Claflin, J.-C. Gérard, and B. Hubert (2002), Proton aurora in the cusp, *J. Geophys. Res.*, *107*(A7), 1091, doi:10.1029/2001JA900161.

Frey, H. U., O. Amm, C. C. Chaston, S. Fu, G. Haerendel, L. Juusola, T. Karlsson, B. Lanchester, R. Nakamura, N. Østgaard, T. Sakanoi, E. Séran, D. Whiter, J. Weygand, K. Asamura, and M. Hirahara (2010), Small and meso-scale properties of a substorm onset auroral arc, *J. Geophys. Res.*, *115*, A10209, doi:*10.1029/2010JA015537*.

Fukunishi, H. (1975), Dynamic relationship between proton and electron substorms, *J. Geophys. Res.*, *80*, 553−574.

Fuselier, S. A., S. B. Mende, T. E. Moore, H. U. Frey, S. B. Petrinec, E. S. Claflin, and M. R. Collier (2003), Cusp dynamics and ionospheric outflow, *Space Sci. Rev.*, *109*, 285–312.

Gallardo-Lacourt, B., Y. Nishimura, L. R. Lyons, S. Zou, V. Angelopoulos, E. Donovan, K. A. McWilliams, J. M. Ruohoniemi, and N. Nishitani (2014), Coordinated SuperDARN THEMIS ASI observations of mesoscale flow bursts associated with auroral streamers, *J. Geophys. Res. Space Phys.*, *119*, 142–150.

Goertz, C. K., and R. W. Boswell (1979), Magnetosphere-Ionosphere coupling, *J. Geophys. Res.*, *84*, 7239.

Gurnett, D. A., and L. A. Frank (1973), Observed relationships between electric fields and auroral particle precipitation, *J. Geophys. Res.*, *78*, 145.

Hallinan, T. J., and T. N. Davis (1970), Small-scale auroral arc distortions, *Planet. Space Sci.*, *18*, 1735.

Horne, R. B., R. M. Thorne, N. P. Meredith, and R. R. Anderson (2003), Diffuse auroral electron scattering by electron cyclotron harmonic and whistler mode waves during an isolated substorm, *J. Geophys. Res.*, *108*, 1290.

Hu, Z.-J., H.-G. Yang, H.-Q. Hu, B.-C. Zhang, D.-H. Huang, Z.-T. Chen, and Q. Wang (2013), The hemispheric conjugate observation of postnoon "bright spots"/auroral spirals, *J. Geophys. Res. Space Phys.*, *118*, 1428–1434.

Hubert, B., J.-C. Gérard, S.-A. Fuselier, S.-B. Mende, and J.-L. Burch (2004), Proton precipitation during transpolar arc events: Observations with the IMAGE-FUV imagers, *J. Geophys. Res.*, *109*, A06204, doi:10.1029/2003JA010136.

Iijima, T., and T. A. Potemra (1976), The amplitude distribution of field-aligned currents at northern high latitudes observed by Triad, *J. Geophys. Res.*, *81*(13), 2165–2174.

Ivchenko, N., E. M. Blixt, and B. S. Lanchester (2005), Multispectral observations of auroral rays and curls, *Geophys. Res. Lett.*, *32*, L18106, doi:10.1029/2005GL022650.

Jayachandran, P. T., N. Sato, Y. Ebihara, A. S. Yukimatu, A. Kadokura, J. W. MacDougall, E. F. Donovan, and K. Liou (2008), Oscillations of the equatorward boundary of the ion auroral oval – radar observations, *J. Geophys. Res.*, *113*, A08208, doi:10.1029/2007JA012870.

Jiang, F., R. J. Strangeway, M. G. Kivelson, J. M. Weygand, R. J. Walker, K. K. Khurana, T. Nishimura, V. Angelopoulos, and E. F. Donovan (2012), In-situ observations of the "preexisting auroral arc" by THEMIS All Sky Imagers and the FAST spacecraft, *J. Geophys. Res.*, doi:10.1029/2011JA017128.

Johnstone, A. D., and J. D. Winningham (1982), Satellite observations of suprathermal electron bursts, *J. Geophys. Res.*, *87*, 2321.

Jorjio, N. V. (1959), Electrophotometrical measurements in the auroral zone, in V. I. Krassovsky (ed.), *Spectral, Electrophotometrical and Radar Research of Aurora and Airglow*, no. 1, Moscow: Academy of Sciences, 30−40.

Kataoka, R., Y. Miyoshi, T. Sakanoi, A. Yaegashi, K. Shiokawa, and Y. Ebihara (2011), Turbulent microstructures and formation of folds in auroral breakup arc, *J. Geophys. Res.*, *116*, A00K02, doi:10.1029/2010JA016334.

Kennel, C. F., and H. E. Petschek (1966), Limit on stably trapped particle fluxes, *J. Geophys. Res.*, *71*(1), 1–28.

Kletzing, C. A., and S. Hu (2001), Alfvén wave generated electron time dispersion, *Geophys. Res. Lett.*, *28*, 693.

Knight, S. (1973), Parallel electric fields, *Planet. Space Sci.*, *21*, 741.

Knudsen, D. J., J. H. Clemmons, and J.-E. Wahlund (1998), Correlation between core ion energization, suprathermal electron beams, and broadband ELF plasma waves, *J. Geophys. Res.*, *103*, 4171.

Kullen, A., M. Brittnacher, J. A. Cumnock, and L. G. Blomberg (2002), Solar wind dependence of the occurrence and motion of polar auroral arcs: A statistical study, *J. Geophys. Res.*, *107*(A11), 1362.

Lin, C. S., and R. A. Hoffman (1979), Characteristics of the inverted-V event, *J. Geophys. Res.*, *84*(A4), 1514–1524.

Liou, K., P. T. Newell, C.-I. Meng, A. T. Y. Lui, M. Brittnacher, and G. Parks (1997), Dayside auroral activity as a possible precursor of substorm onsets: A survey using Polar ultraviolet imagery, *J. Geophys. Res.*, *102*, 19,835–19,843.

Liu, W. W., J. Liang, E. F. Donovan, T. Trondsen, G. Baker, G. Sofko, B. Jackel, C.-P. Wang, S. Mende, H. U. Frey, and V. Angelopoulos (2008), Observation of isolated high-speed auroral streamers and their interpretation as optical signatures of Alfvén waves generated by bursty bulk flows, *Geophys. Res. Lett.*, *35*, L04104, doi:10.1029/2007GL032722.

Luhr, H., and K. Schlegel (1994), Combined measurements of EISCAT and the EISCAT magnetometer cross to study omega bands, *J. Geophys. Res.*, *99*(A5), 8951–8959.

Lui, A. T. Y., D. Venkatesan, C. D. Anger, S.-I. Akasofu, W. J. Heikkila, J. D. Winningham, and J. R. Burrows (1977), Simultaneous observations of particle precipitations and auroral emissions by the Isis 2 satellite in the 19–24 MLT sector, *J. Geophys. Res.*, *82(*16), 2210–2226.

Luízar, O., M. V. Stepanova, J. M. Bosqued, E. E. Antonova, and R. A. Kovrazhkin (2000), Experimental study of the formation of inverted-V structures and their stratification using AUREOL-3 observations, *Annales Geophysicae*, *18*(11), 1399−1411.

Lynch, K. A., R. L. Arnoldy, P. M. Kintner, and J. L. Vago (1994), Electron distribution function behavior during localized transverse ion acceleration events in the topside auroral zone, *J. Geophys. Res.*, *99*, 2227.

Lynch, K. A., D. Pietrowski, R. B. Torbert, N. Ivchenko, G. Marklund, and F. Primdahl (1999), Multiple-point electron measurements in a nightside auroral arc: Auroral Turbulence II particle observations, *Geophys. Res. Lett.*, *26*, 3361.

Lyons, L. R. (1981), Discrete aurora as the direct result of an inferred high-altitude generating potential distribution, *J. Geophys. Res.*, *86*(A1), 1–8.

Lyons, L. R., and R. L. Walterscheid (1985), Generation of auroral omega bands by shear instability of the neutral winds, *J. Geophys. Res.*, *90*(A12), 12321–12329.

Lyons, L. R., T. Nagai, G. T. Blanchard, J. C. Samson, T. Yamamoto, T. Mukai, A. Nishida, and S. Kokobun (1999), Association between Geotail plasma flows and auroral poleward boundary intensifications observed by CANOPUS photometers, *J. Geophys. Res.*, *104*, 4485–4500.

Lyons, L. R., Y. Nishimura, H.-J. Kim, E. Donovan, V. Angelopoulos, G. Sofko, M. Nicolls, C. Heinselman, J. M. Ruohoniemi, and N. Nishitani (2011), Possible connection of polar cap flows to pre- and post-substorm onset PBIs and streamers, *J. Geophys. Res.*, *116*, A12225, doi:10.1029/2011JA016850.

Lysak, R. L. (1998), The relationship between electrostatic shocks and kinetic Alfvén waves, *Geophys. Res. Lett.*, *25*, 2089.

Lysak, R. L., and W. Lotko (1996), On the kinetic dispersion relation for shear Alfvén waves, *J. Geophys. Res.*, *101*, 5085.

Lysak, R. L., and Y. Song (1996), Coupling of Kelvin-Helmholtz and current sheet instabilities to the ionosphere: A dynamic theory of auroral spirals, *J. Geophys. Res.*, *101*(A7), 15411–15422.

Lysak, R. L., and Y. Song (2003), Kinetic theory of the Alfvén wave acceleration of auroral electrons, *J. Geophys. Res.*, *108*(A4), 8005.

Marklund, G., L. Blomberg, C. G. Falthammar, and P. A. Lindqvist (1994), On intense diverging electric fields associated with black aurora, *Geophys. Res. Lett.*, *21*, 1859–1862.

Marklund, G., T. Karlsson, and J. Clemmons (1997), On low-altitude particle acceleration and intense electric fields and their relationship to black aurora, *J. Geophys. Res.*, *102*, 17,509–17,522.

Marklund, G. T., T. Karlsson, L. G. Blomberg, P.-A. Lindqvist, C.-G. Fälthammar, M. L. Johnson, J. S. Murphree, L. Andersson, L. Eliasson, H. J. Opgenoorth, and L. J. Zanetti (1998), Observations of the electric field fine structure associated with the westward traveling surge and large-scale auroral spirals, *J. Geophys. Res.*, 103(A3), 4125–4144, doi:10.1029/97JA00558.

Marklund, G. T., S. Sadeghi, J. A. Cumnock, T. Karlsson, P.-A. Lindqvist, H. Nilsson, A. Masson, A. Fazakerley, E. Lucek, J. Pickett, and Y. Zhang (2011), Evolution in space and time of the quasi-static acceleration potential of inverted-V aurora and its interaction with Alfvénic boundary processes, *J. Geophys. Res.*, *116*, A00K13, doi:10.1029/2011JA016537.

McFadden, J. P., C. W. Carlson, and M. H. Boehm (1986), Field-aligned electron precipitation at the edge of an arc, *J. Geophys. Res.*, *91*, 1723.

McFadden, J. P., C. W. Carlson, R. E. Ergun, F. S. Mozer, M. Temerin, W. Peria, D. M. Klumpar, E.G. Shelley, W. K. Peterson, E. Moebius, L. Kistler, R. Elphic, R. Strangeway, C. Cattell, and R. Pfaff (1998), Spatial structure and gradients of ion beams observed by FAST, *Geophys. Res. Lett.*, *25*, 2021.

McFadden, J. P., C. W. Carlson, and R. E. Ergun (1999), Microstructure of the auroral acceleration region as observed by FAST, *J. Geophys. Res.*, *104*(A7), 14453–14480.

McPherron, R. L. (1970), Growth phase of magnetospheric substorms, *J. Geophys. Res.*, *75*, 5592−5599.

McPherron, R. L. (1972), Substorm related changes in the geomagnetic tail: The growth phase, *Planet. Space Sci.*, *20*, 1521−1539.

Mende, S. B., C. Carlson, H. U. Frey, T. J. Immel, and J.-C. Gerard (2002), IMAGE FUV and in-situ FAST particle observations of substorm aurorae, *J. Geophys. Res.*, *108*(A4), 8010.

Mende, S. B., C. W. Carlson, H. U. Frey, L. M. Peticolas, and N. Ostgaard (2003), FAST and IMAGE-FUV observations of a substorm onset, *J. Geophys. Res.*, *108*(A9), 1344.

Mende, S. B., H. U. Frey, V. Angelopoulos, and Y. Nishimura (2011), Substorm triggering by poleward boundary intensification and related equatorward propagation, *J. Geophys. Res.*, *116*, A00I31, doi:10.1029/2010JA015733.

Meng, C.-I. (1979), Diurnal variation of the auroral oval size, *J. Geophys. Res.*, *84*(A9), 5319–5324.

Meredith, N. P., R. B. Horne, R. M. Thorne, and R. R. Anderson (2009), Survey of upper band chorus and ECH waves: Implications for the diffuse aurora, *J. Geophys. Res.*, *114*, A07218, doi:10.1029/2009JA014230.

Milan, S. E., M. Lester, S. W. H. Cowley, and M. Brittnacher (2000), Dayside convection and auroral morphology during an interval of north-ward interplanetary magnetic field, *Ann. Geophys.*, *18*, 436–444.

Milan, S. E., J. Hutchinson, P. D. Boakes, and B. Hubert (2009), Influences on the radius of the auroral oval, *Ann. Geophys.*, *27*, 2925–2936.

Mozer, F. S., and U. V. Fahleson (1970), Parallel and perpendicular electric fields in the auroral ionosphere, *Planet. Space Sci.*, *18*, 1563.

Mozer, F. S., C. W. Carlson, M. K. Hudson, R. B. Torbert, B. Parady, J. Yatteau, and M. C. Kelley (1977), Observations of paired electrostatic shocks in the polar magnetosphere, *Phys. Rev. Lett.*, *38*, 292.

Mozer, F. S., C. A. Cattell, M. K. Hudson, R. L. Lysak, M. Temerin, and R. B. Torbert (1980), Satellite measurements and theories of auroral particle acceleration, *Space Sci. Rev.*, *27*, 155.

Mozer, F. S., and C. A. Kletzing (1998), Direct observation of large, quasi-static, parallel electric fields in the auroral acceleration region, *Geophys. Res. Lett.*, *25*, 1629.

Mozer, F. S., and A. Hull (2001), Origin and geometry of upward parallel electric fields in the auroral acceleration region, *J. Geophys. Res.*, *106*, 5763.

Naehr, S. M., and F. R. Toffoletto (2004), Quantitative modeling of the magnetic field configuration associated with the theta aurora, *J. Geophys. Res.*, *109*, A07202, doi:10.1029/2003JA010191.

Nakajima, A., K. Shiokawa, K. Seki, R. J. Strangeway, J. P. McFadden and C. W. Carlson (2007), Particle and field characteristics of broadband electrons observed by the FAST satellite during a geomagnetic storm, *J. Geophys. Res.*, *112*, A06220, doi:10.1029/2006JA012184.

Nakamura, R., T. Oguti, T. Yamamoto, and S. Kokubun (1993), Equatorward and poleward expansion of the auroras during auroral substorms, *J. Geophys. Res.*, *98*(A4), 5743–5759.

Nakamura, R., W. Baumjohann, R. Schödel, M. Brittnacher, V. A. Sergeev, M. Kubyshkina, T. Mukai, and K. Liou (2001), Earthward flow bursts, auroral streamers, and small expansions, *J. Geophys. Res.*, *106*(A6), 10791–10802.

Newell, P. T. (2003), A new dawn for aurora, *Nature*, *424*, 734–735.

Newell, P. T., T. Sotirelis, and E. J. Mitchell (2012), Evolution of auroral acceleration types inferred from two-satellite coincidences, *J. Geophys. Res.*, *117*, A12216, doi:10.1029/2012JA018287.

Nishimura, Y., L. Lyons, S. Zou, V. Angelopoulos, and S. Mende (2010), Substorm triggering by new plasma intrusion: THEMIS all-sky imager observations, *J. Geophys. Res.*, *115*, A07222, doi:10.1029/2009JA015166.

Nishimura, Y., L. R. Lyons, V. Angelopoulos, T. Kikuchi, S. Zou, and S. B. Mende (2011), Relations between multiple auroral streamers, pre-onset thin arc formation, and substorm auroral onset, *J. Geophys. Res.*, *116*, A09214, doi:10.1029/2011JA016768.

Nishimura, Y., L. R. Lyons, T. Kikuchi, V. Angelopoulos, E. Donovan, S. Mende, P. J. Chi, and T. Nagatsuma (2012), Formation of substorm Pi2: A coherent response to auroral streamers and currents, *J. Geophys. Res.*, *117*, A09218, doi:10.1029/2012JA017889.

Nishimura, Y., J. Bortnik, W. Li, R. M. Thorne, B. Ni, L. R. Lyons, V. Angelopoulos, Y. Ebihara, J. W. Bonnell, O. Le Contel, and U. Auster (2013a), Structures of dayside whistler-mode waves deduced from conjugate diffuse aurora, *J. Geophys. Res. Space Phys.*, *118*, 664–673, doi:10.1029/2012JA018242.

Nishimura, Y., L. R. Lyons, K. Shiokawa, V. Angelopoulos, E. F. Donovan, and S. B. Mende (2013b), Substorm onset and expansion phase intensification precursors seen in polar cap patches and arcs, *J. Geophys. Res. Space Phys.*, *118*, doi:10.1002/jgra.50279.

Opgenoorth, H. J., J. Oksman, K. U. Kaila, E. Nielsen, and W. Baumjohann (1983), Characteristics of eastward drifting omega bands in the morning sector of the auroral oval, *J. Geophys. Res.*, *88*(A11), 9171–9185.

Partamies, N., K. Kauristie, T. I. Pulkkinen, and M. Brittnacher (2001), Statistical study of auroral spirals, *J. Geophys. Res.*, *106*(A8), 15415–15428.

Paschmann, G. (2003), *Auroral Plasma Physics*, Dordrecht: Kluwer Academic Publishers.

Peticolas, L. M., T. J. Hallinan, H. C. Stenbaek-Nielsen, J. W. Bonnell, and C. W. Carlson (2002), A study of black aurora from aircraft-based optical observations and plasma measurements on FAST, *J. Geophys. Res.*, *107*(A8), doi:10.1029/2001JA900157.

Rostoker, G., S.-I. Akasofu, J. Foster, R. Greenwald, Y. Kamide, K. Kawasaki, A. Lui, R. McPherron, and C. Russell (1980), Magnetospheric substorms—definition and signatures, *J. Geophys. Res.*, *85*(A4), 1663–1668.

Sadeghi, S., G. T. Marklund, T. Karlsson, P.-A. Lindqvist, H. Nilsson, O. Marghitu, A. Fazakerley, and E. A. Lucek (2011), Spatiotemporal features of the auroral acceleration region as observed by Cluster, *J. Geophys. Res.*, *116*, A00K19, doi:10.1029/2011JA016505.

Sandholt, P. E., C. J. Farrugia, J. Moen, Ø. Noraberg, B. Lybekk, T. Sten, and T. Hansen (1998), A classification of dayside auroral forms and activities as a function of interplanetary magnetic field orientation, *J. Geophys. Res.*, *103*(A10), 23325–23345.

Seyler, C. E., and K. Liu (2007), Particle energization by oblique inertial Alfvén waves in the auroral region, *J. Geophys. Res.*, *112*, A09302, doi:10.1029/2007JA012412.

Singh, N., and J. L. Horwitz (1992), Plasmasphere refilling: Recent observations and modeling, *J. Geophys. Res.*, *97*, 1049–1079.

Siscoe, G. L., G. M. Erickson, B. U. O. Sonnerup, N. C. Maynard, K. D. Siebert, D. R. Weimer, and W. W. White (2001), Global role of $E_{||}$ in magnetopause reconnection: An explicit demonstration, *J. Geophys. Res.*, *106*, 13,015–13,022.

Stenbaek-Nielsen, H., T. Hallinan, D. Osborne, J. Kimball, C. Chaston, J. McFadden, G. Delory, M. Temerin, and C. Carlson (1998), Aircraft observations conjugate to FAST, *Geophys. Res. Lett.*, *25*, 2073–2076.

Thorne, R. M., B. Ni, X. Tao, R. B. Horne, and N. P. Meredith (2010), Scattering by chorus waves as the dominant cause of diffuse auroral precipitation. *Nature*, *467* (7318), 943 doi:10.1038/nature09467

Trondsen, T. S., and L. L. Cogger (1997), High-resolution television observations of black aurora, *J. Geophys. Res.*, *102*, 363–378.

Vogt, J., H. U. Frey, G. Haerendel, H. Höfner, and J. L. Semeter (1999), Shear velocity profiles associated with auroral curls, *J. Geophys. Res.*, *104*(A8), 17277–17288.

Wagner, J. S., R. D. Sydora, T. Tajima, T. Hallinan, L. C. Lee, and S.-I. Akasofu (1983), Small-scale auroral arc deformations, *J. Geophys. Res.*, *88*(A10), 8013–8019.

Whipple, E. C., Jr. (1977), The signature of parallel electric fields in a collisionless plasma, *J. Geophys. Res.*, *82*, 1525.

Wild, J. A., E. E. Woodfield, E. Donovan, R. C. Fear, A. Grocott, M. Lester, A. N. Fazakerley, E. Lucek, Y. Khotyaintsev, M. Andre, A. Kadokura, K. Hosokawa, C. Carlson, J. P. McFadden, K. H. Glassmeier, V. Angelopoulos, and G. Björnsson (2011), Midnight sector observations of auroral omega bands, *J. Geophys. Res.*, *116*, A00I30, doi:10.1029/2010JA015874.

Wygant, J. R., A. Keiling, C. A. Cattell, M. Johnson, R. L. Lysak, M. Temerin, F. S. Mozer, C. A. Kletzing, J. D. Scudder, W. Peterson, C. T. Russell, G. Parks, M. Brittnacher, G. Germany, and J. Spann (2000), Polar spacecraft based comparisons of intense electric fields and Poynting flux near and within the plasma sheet-tail lobe boundary to UVI images: An energy source for the aurora, *J. Geophys. Res.*, *105*, 18,675.

Wygant, J. R., A. Keiling, C. A. Cattell, R. L. Lysak, M. Temerin, F. S. Mozer, C. A. Kletzing, J. D. Scudder, V. Streltsov, W. Lotko, and C. T. Russell (2002), Evidence for kinetic Alfvén waves and parallel electron energization at 4-6 RE altitudes in the plasma sheet boundary layer, *J. Geophys. Res.*, *107*, 1201, doi:10.1029/2001JA900113.

Yamamoto, T., S. Inoue, and C.-I. Meng (1997), Formation of auroral omega bands in the paired region 1 and region 2 field-aligned current system, *J. Geophys. Res.*, *102*(A2), 2531–2544.

Yue, C., Y. Nishimura, L. R. Lyons, V. Angelopoulos, E. F. Donovan, Q. Shi, Z. Yao, and J. W. Bonnell (2013), Coordinated THEMIS spacecraft and all-sky imager observations of interplanetary shock effects on plasma sheet flow bursts, poleward boundary intensifications, and streamers, *J. Geophys. Res. Space Phys.*, *118*, 3346–3356.

Zhang, Y., L. J. Paxton, T. J. Immel, H. U. Frey, and S. B. Mende (2002), Sudden solar wind dynamic pressure enhancements and dayside detached auroras: IMAGE and DMSP observations, *J. Geophys. Res.*, *107*, 8001, doi:10.1029/2002JA009355 [printed *108*(A4), 2003].

Zou, S., M. B. Moldwin, L. R. Lyons, Y. Nishimura, M. Hirahara, T. Sakanoi, K. Asamura, M. J. Nicolls, Y. Miyashita, S. B. Mende, and C. J. Heinselman (2010), Identification of substorm onset location and preonset sequence using Reimei, THEMIS GBO, PFISR, and Geotail, *J. Geophys. Res.*, *115*, A12309, doi:10.1029/2010JA015520.